

# Assessment of Perfusion Pattern and Extent of Perfusion Defect on Dual-Energy CT Angiography: Correlations between the Causes of Pulmonary Hypertension and Vascular Parameters

Eun Young Kim, MD<sup>1,2</sup>, Joon Beom Seo, MD, PhD<sup>2</sup>, Sang Young Oh, MD<sup>2</sup>, Choong Wook Lee, MD<sup>2</sup>, Hye Jeon Hwang, MD<sup>3</sup>, Sang Min Lee, MD<sup>2</sup>, Young Kyung Lee, MD, PhD<sup>4</sup>

<sup>1</sup>Department of Radiology, Chonbuk National University Medical School and Hospital, Research Institute of Clinical Medicine, Jeonju 561-712, Korea; <sup>2</sup>Department of Radiology and Research Institute of Radiology, University of Ulsan College of Medicine, Asan Medical Center, Seoul 138-736, Korea; <sup>3</sup>Department of Radiology, Hallym University College of Medicine, Hallym University Sacred Heart Hospital, Anyang 431-796, Korea; <sup>4</sup>Department of Radiology, Seoul Medical Center, Seoul 131-865, Korea

**Objective:** To assess perfusion patterns on a dual-energy pulmonary CT angiography (DECTA) of pulmonary hypertension (PHT) with variable causes and to assess whether the extent of perfusion defect can be used in the severity assessment of PHT.

**Materials and Methods:** Between March 2007 and February 2011, DECTA scans of 62 consecutive patients (24 men, 38 women; mean age,  $58.5 \pm 17.3$  [standard deviation] years; range, 19–87 years) with PHT were retrospectively included with following inclusion criteria; 1) absence of acute pulmonary thromboembolism, 2) maximal velocity of tricuspid regurgitation jet (TR Vmax) above 3 m/s on echocardiography performed within one week of the DECTA study. Perfusion patterns of iodine map were divided into normal (NL), diffuse heterogeneously decreased (DH), multifocal geographic and multiple peripheral wedging patterns. The extent of perfusion defects (PD), the diameter of main pulmonary artery (MPA) and the ratio of ascending aorta diameter/MPA (aortopulmonary ratio, APR) were measured. Pearson correlation analysis was performed between TR Vmax on echocardiography and CT imaging parameters.

**Results:** Common perfusion patterns of primary PHT were DH ( $n = 15$ ) and NL ( $n = 12$ ). The perfusion patterns of secondary PHT were variable. On the correlation analysis, in primary PHT, TR Vmax significantly correlated with PD, MPA and APR ( $r = 0.52$ ,  $r = 0.40$ ,  $r = -0.50$ , respectively, all  $p < 0.05$ ). In secondary PHT, TR Vmax significantly correlated with PD and MPA ( $r = 0.38$ ,  $r = 0.53$ , respectively, all  $p < 0.05$ ).

**Conclusion:** Different perfusion patterns are observed on DECTA of PHT according to the causes. PD and MPA are significantly correlated with the TR Vmax.

**Index terms:** Pulmonary hypertension; Dual-energy CT; Pulmonary perfusion

Received June 26, 2013; accepted after revision January 10, 2014.  
This study was supported by a grant of the Korean Health Technology R&D Project, Ministry of Health & Welfare, Republic of Korea (A111599).

**Corresponding author:** Joon Beom Seo, MD, PhD, Department of Radiology and Research Institute of Radiology, University of Ulsan College of Medicine, Asan Medical Center, 88 Olympic-ro 43-gil, Songpa-gu, Seoul 138-736, Korea.

• Tel: (822) 3010-4383 • Fax: (822) 476-4719

• E-mail: seojb@amc.seoul.kr

This is an Open Access article distributed under the terms of the Creative Commons Attribution Non-Commercial License (<http://creativecommons.org/licenses/by-nc/3.0>) which permits unrestricted non-commercial use, distribution, and reproduction in any medium, provided the original work is properly cited.

## INTRODUCTION

Pulmonary hypertension (PHT) is one of the most serious chronic disorders of the pulmonary circulation; it can cause right ventricular failure and even death. Because most patients tend to initially present with non-specific symptoms, they are usually diagnosed with PHT at a late stage, thus resulting in high mortality and morbidity. Therefore, it is important to discover potentially curable forms of PHT as early as possible. There have been several studies reported analyzing the perfusion patterns and determining the causes of PHT using pulmonary perfusion

scintigraphy (1, 2). Abnormal radiotracer distribution in patients with PHT may be caused by some different mechanisms. One mechanism is arterial thromboembolic occlusion such as in chronic thromboembolic pulmonary hypertension (CTEPH). Another mechanism is parenchymal destruction such as in interstitial lung disease and emphysema or by distal arteriopathy such as in idiopathic PHT and other nonembolic forms (3, 4). A different imaging pattern is resulting from these mechanisms. However, the perfusion patterns of perfusion scans were only useful for the distinction between embolic and non-embolic causes and were not helpful for the distinction of histologic subtypes, primarily because of its limited spatial resolution. Although right-heart catheterization remains the gold standard for correct diagnosing of PHT (5), a superb noninvasive way to check the suspected PHT patients is the transthoracic Doppler echocardiography. Maximal velocity of tricuspid regurgitation jet (TR Vmax) has linear positive and negative correlations with systolic pulmonary arterial pressure and mean pulmonary arterial pressure measured by right-heart catheterization (6-10).

High-resolution computed tomography (CT) and CT angiography play a crucial role in the diagnostic work-up of PHT (11) as they show higher a sensitivity and specificity than lung perfusion scintigraphy for the evaluation of patients with PHT caused by various etiologies, particularly in patients with CTEPH (3, 12). Many attempts have been made to establish reliable and reproducible evaluation methods for the assessment of PHT severity using CT. Earlier results have shown that an increase in the diameter of the main pulmonary artery (PA) is a reliable indicator of PHT (13). The ratio of diameter of PA to the diameter of the ascending aorta (aortopulmonary ratio, APR) and the diameter of the segmental PA compared to that of the homologous segmental bronchus have also been investigated in order to predict the severity of PHT (14, 15). However, measuring the main PA diameter or the APR in order to predict the severity of PHT remains controversial. Recently, assessments of the lung-perfused blood volume (LPBV) or pulmonary perfusion have been made using contrast-enhanced dual-energy CT (DECT) in patients with acute pulmonary thromboembolism (PTE) (16-20). Although there were several studies about the evaluation of the diagnostic utility of LPBV for CTEPH (21-23), no studies were conducted yet to evaluate PHT of various causes other than CTEPH. The purpose of the present study was to assess the perfusion pattern seen on dual-energy pulmonary CT

angiography (DECTA) of PHT with various causes and to investigate whether the extent of the perfusion defect can be used in the severity assessment of PHT.

## MATERIALS AND METHODS

### Patients

This retrospective study was approved by our Institutional Review Board and an informed consent was waived.

Between March 2007 and February 2011, 120 patients underwent DECTA with the clinical suspicion of PTE. The patients were included, whose TR Vmax was above 3 m/s on echocardiography. The echocardiography was performed within one week after the DECTA study. Of these patients, 58 patients with clinical diagnosis of acute PTE were excluded. Therefore, 62 patients (24 men, 38 women; mean age, 58.5 ± 17.3 [standard deviation, SD] years; range 19–87 years) comprised our study population. Right-heart catheterization was performed in 8 patients of total 62 patients.

### Scan and Contrast Injection Protocol

CT scans were performed using a DECT protocol recommended by the manufacturer of the two types of dual-source scanners (Somatom Definition [ $n = 56$ ] and Somatome Definition Flash [ $n = 6$ ] scanner, Siemens Healthcare, Forchheim, Germany). For example, the protocol for the Somatom Definition was as follows: 512 × 512 matrix; 14 × 1.2 mm collimation; 50 effective mAs at 140 kV and 210 effective mAs at 80 kV; 0.5 pitch and 0.33-second rotation time. Images were acquired in a single breath-hold in the craniocaudal direction from the lung apex to the costophrenic angles. A power injector was used to administer 100 mL of iodine contrast material (iopromide, Ultravist 370, Bayer Schering Pharma, Berlin, Germany) at a rate of 3.5 mL/s. A fixed scan delay of 20 seconds was used.

### Perfusion Image Generation

Data from the 80 kV, 140 kV and weighted average images were transferred to a workstation (MultiModality Workplace, Siemens Healthcare, Forchheim, Germany). The weighted average images were automatically generated from a combination of the 140 and 80 kV data with a weighting factor of 1:4 (140:80 kV). These weighted average images were used as conventional pulmonary CT angiographic images. A color-coded iodine image based on the material decomposition theory was obtained using

the LPBV application of the workstation software (Syngo Dual Energy). The application class was designed for iodine extraction and the material parameters for iodine extraction were as follows: -1000 Hounsfield units (HU) for air at 80 kV; -1000 HU for air at 140 kV; 60 HU for soft tissue at 80 kV; 54 HU for soft tissue at 140 kV, 2 for relative contrast enhancement; -960 HU for minimum value; -300 HU for maximum value and 4 for range. A color-coded image with a rainbow color setting was used as perfusion image where the red color indicates the highest iodine enhancement and the violet color the lowest enhancement. The window settings of the perfusion image were fixed to a level of

50 HU and a width of 100 HU. Only data displayed inside the dual-energy field of view (FOV) were used for the dual-energy evaluation.

**Image Analysis**

Based on the clinical features and image findings, the patients were classified as primary and secondary PHT. The secondary PHT was further subdivided into four groups according to the cause of PHT, i.e., cardiogenic, vascular, chronic obstructive pulmonary disease (COPD) and interstitial lung disease. Vascular causes included chronic thromboembolism, vascular occlusion due to fibrosing

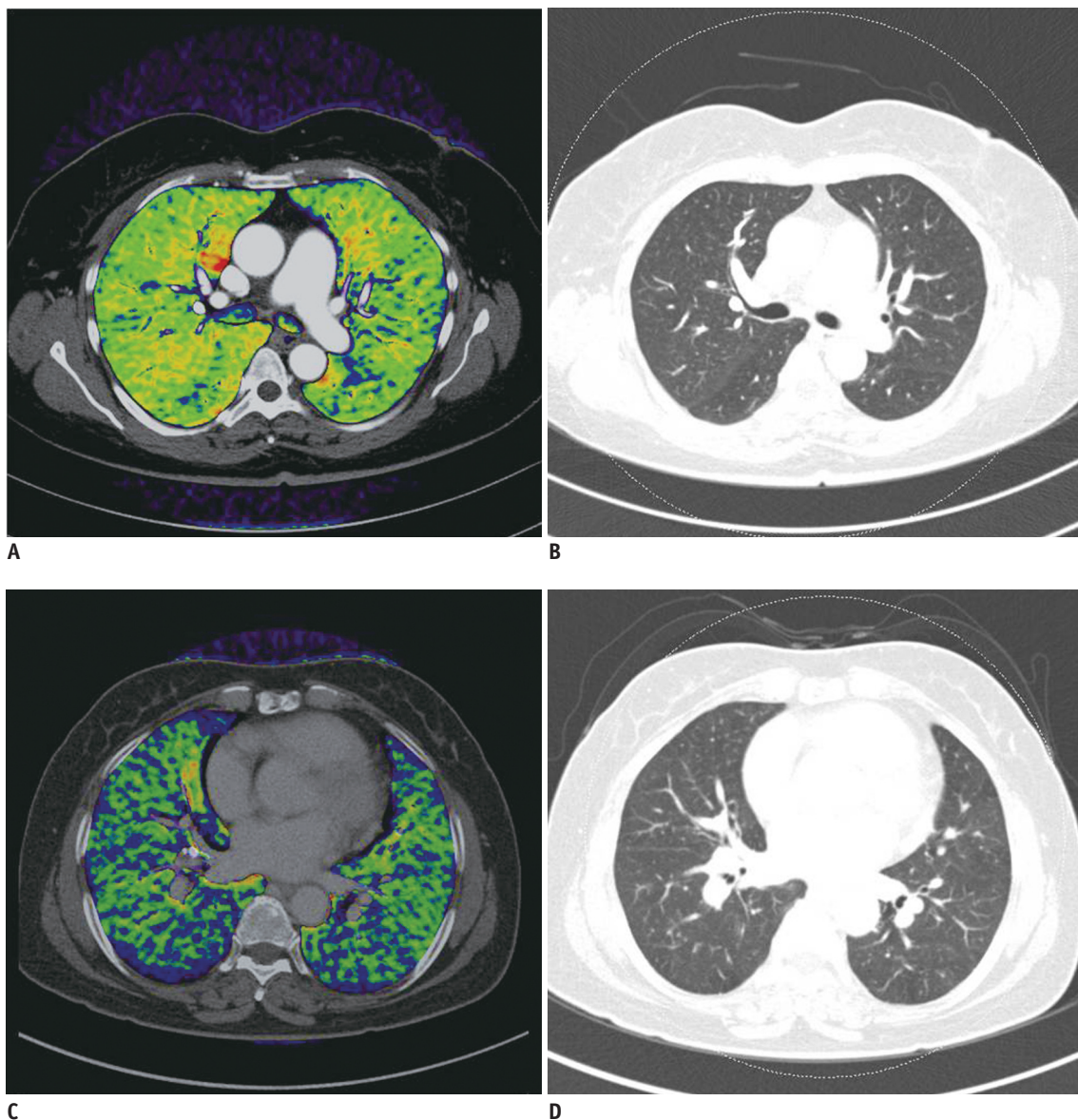


**Fig. 1. Examples showing four different types of perfusion patterns and parenchymal lung images in various causes of PHT.** They are color-coded perfusion images and lung setting images in 4 patients diagnosed with PHT. **A, B.** 42-year-old woman diagnosed with primary PHT shows normal perfusion pattern with normal lung parenchyma. **C, D.** 65-year-old woman with primary PHT shows diffuse heterogeneously decreased pattern with normal lung parenchyma. PHT = pulmonary hypertension



mediastinitis, and Takayasu's arteritis.

Two reviewers blinded to the conventional pulmonary CTA findings independently assessed the perfusion patterns and visually assessed the extent of perfusion defect (PD) of the iodine map. Normal perfusion was seen as red to yellow color, moderately decreased perfusion as green to blue, and no perfusion as dark blue to black on the color-coded perfusion images.

According to its morphology the perfusion pattern of the iodine map was categorized into four classes: normal (NL), no perfusion defect; diffuse heterogeneously decreased

(DH), heterogeneous perfusion defect with intervening areas of preserved perfusion; multifocal geographic (MG), large areas of one color with variably scalloped borders sharply interfaced with another color; and multiple peripheral wedging patterns, a wedge-shaped sharply demarcated perfusion defect in the peripheral area (Fig. 1). Discordant results regarding the perfusion pattern were resolved in consensus during the reading session. The extent of the average perfusion defect was calculated on a 5% scale from three different coronal planes including the ascending aorta, tracheal carina and the vertebra level. The

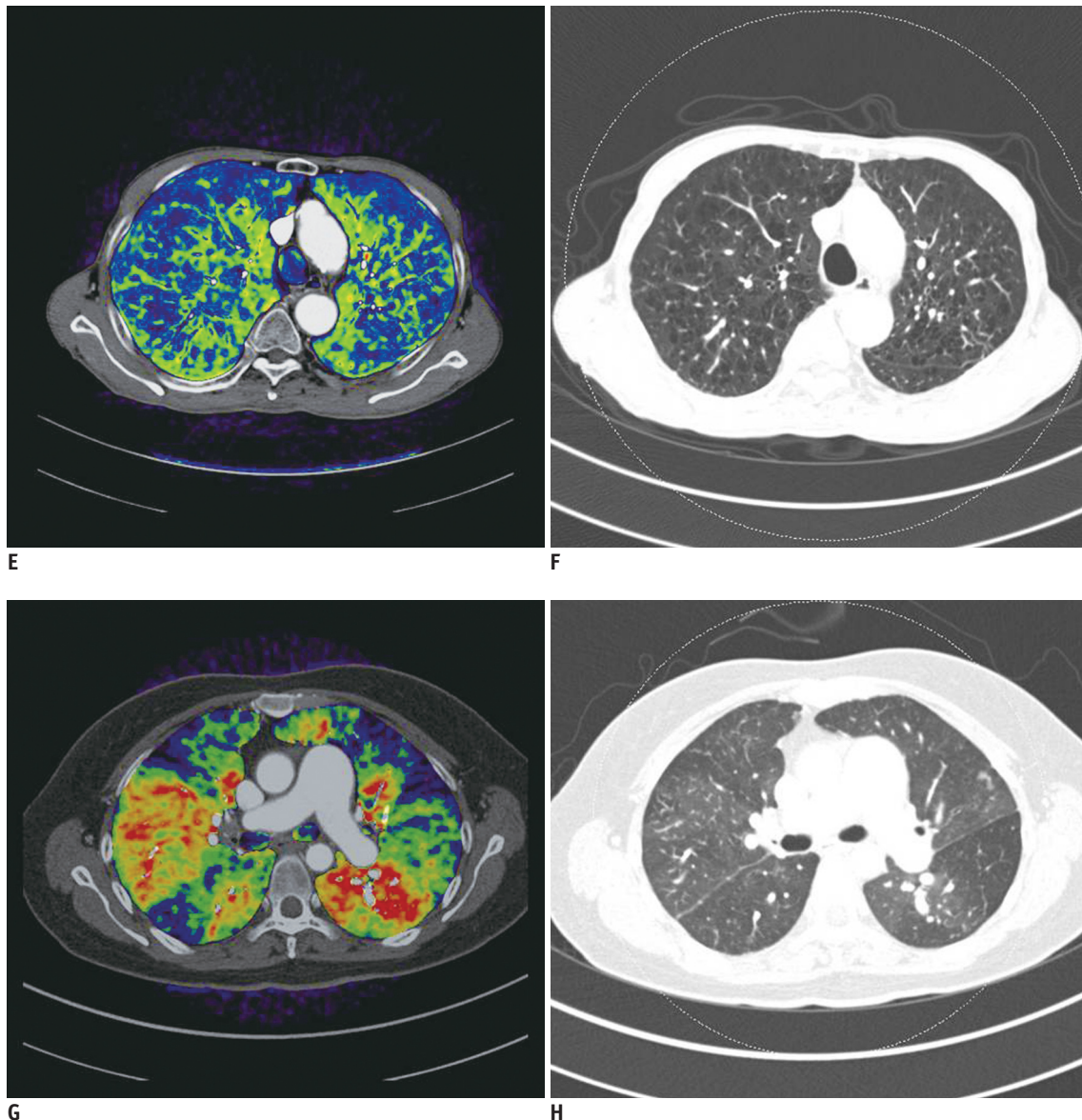


**Fig. 1. Examples showing four different types of perfusion patterns and parenchymal lung images in various causes of PHT.** They are color-coded perfusion images and lung setting images in 4 patients diagnosed with PHT. **E, F.** 87-year-old man with secondary PHT (COPD) shows multifocal geographic pattern with emphysema. **G, H.** 55-year-old woman with secondary PHT (CTEPH) shows multiple peripheral wedging pattern with mosaic attenuation. COPD = chronic obstructive pulmonary disease, CTEPH = chronic thromboembolic pulmonary hypertension, PHT = pulmonary hypertension

widest diameter perpendicular to the long axis of the main PA (MPA) and APR was measured with computer calipers at the level of the pulmonary arterial bifurcation.

### Statistical Analysis

Statistical software packages (SPSS version 19, SPSS Inc., Chicago, IL, USA; MedCalc version 7.3, MedCalc Software, Mariakerke, Belgium) were used. The results were expressed as mean  $\pm$  SD. Agreement between the two readers regarding the perfusion patterns was assessed using kappa statistics. Agreement between the same two readers regarding the extent of the perfusion defect was analyzed using the intraclass correlation coefficient (ICC). Pearson correlation and multiple linear regression analysis were evaluated between TR Vmax on echocardiography and the CT imaging parameters. In addition, Spearman correlation was evaluated between mean pulmonary arterial pressure by right-heart catheterization and PD, MPA and APR. The mean value of both readers' results was used for the correlation analysis. A value of  $p < 0.05$  was considered to indicate statistical significance; all  $p$  values were two-tailed.

## RESULTS

The inter-reader agreement for determining the perfusion pattern on independent reading was moderate with a kappa value of 0.59. The number of patients diagnosed

with primary PHT was 30 and 32 with secondary PHT. The common perfusion patterns of primary PHT were DH ( $n = 15$ ) and NL ( $n = 12$ ). The perfusion patterns of secondary PHT varied according to the causes (Table 1). The common perfusion pattern of secondary PHT was MG ( $n = 14$ ). PD ranged from  $35.8 \pm 22.4\%$  to  $57.9 \pm 10.0\%$  in secondary PHT. The ICC regarding the perfusion defect was 0.91. Regarding the correlation analysis of all patients, TR Vmax significantly correlated with PD, MPA and APR (Table 2, Fig. 2). However, PD did not correlate significantly with either MPA or APR. Multiple linear regression analysis revealed that MPA and PD were independent determinants of TR Vmax ( $R^2 = 0.31$ ) (Table 3). Mean pulmonary arterial pressure by right-heart catheterization significantly correlated with PD ( $r = 0.73$ ,  $p = 0.04$ ), MPA ( $r = 0.35$ ,  $p = 0.40$ ), and APR ( $r = -0.49$ ,  $p = 0.22$ ).

## DISCUSSION

In this study, a different perfusion patterns were observed according to the various causes of PHT thus suggesting the perfusion pattern offers additional information for the PHT cause identification. In addition, the severity of PHT assessed by measuring the extent of the mean perfusion defect on DECT perfusion imaging showed a significant correlation with the TR Vmax. Hoey et al. (21) showed that DECT can offer a "one-stop" assessment

**Table 1. Perfusion Pattern and Extent of Mean Perfusion Defect Analysis on DECT and Mean TR Vmax on Echocardiography According to Cause of PHT**

Cause of PHT	Perfusion Pattern (n)				Extent of Perfusion Defect (Mean %)	TR Vmax (m/s)
	NL	DH	MG	PW		
Primary PHT (n = 30)	12	15	2	1	$37.9 \pm 18.3$	$3.9 \pm 0.1$
Secondary PHT (n = 32)	8	5	14	8	$65.0 \pm 20.0$	$4.7 \pm 0.8$
Cardiogenic (n = 9)	6	2	1		$35.8 \pm 22.4$	$4.5 \pm 1.1$
Vascular (n = 8)			3	5	$48.8 \pm 10.0$	$3.8 \pm 0.0$
COPD (n = 9)			8	1	$57.9 \pm 10.0$	$4.7 \pm 0.1$
ILD (n = 6)	2		2	2	$44.6 \pm 50.0$	$3.9 \pm 0.5$

**Note.**— COPD = chronic obstructive pulmonary disease, DECT = dual-energy CT, DH = diffuse heterogeneously decreased, ILD = interstitial lung disease, MG = multifocal geographic, NL = normal, PHT = pulmonary hypertension, PW = multiple peripheral wedging, TR Vmax = maximal velocity of tricuspid regurgitation jet

**Table 2. Pearson Correlation between TR Vmax and CT Parameters**

Pearson Correlation	PD	MPA	APR
All	$r = 0.35$ ( $p < 0.01$ )	$r = 0.46$ ( $p < 0.01$ )	$r = -0.35$ ( $p < 0.01$ )
Primary PHT	$r = 0.52$ ( $p < 0.01$ )	$r = 0.40$ ( $p < 0.05$ )	$r = -0.50$ ( $p < 0.01$ )
Secondary PHT	$r = 0.38$ ( $p < 0.05$ )	$r = 0.53$ ( $p < 0.01$ )	$r = -0.28$ ( $p = 0.13$ )

**Note.**— APR = aortopulmonary ratio, MPA = diameter of the main pulmonary artery, PD = extent of perfusion defect, PHT = pulmonary hypertension, TR Vmax = maximal velocity of tricuspid regurgitation jet

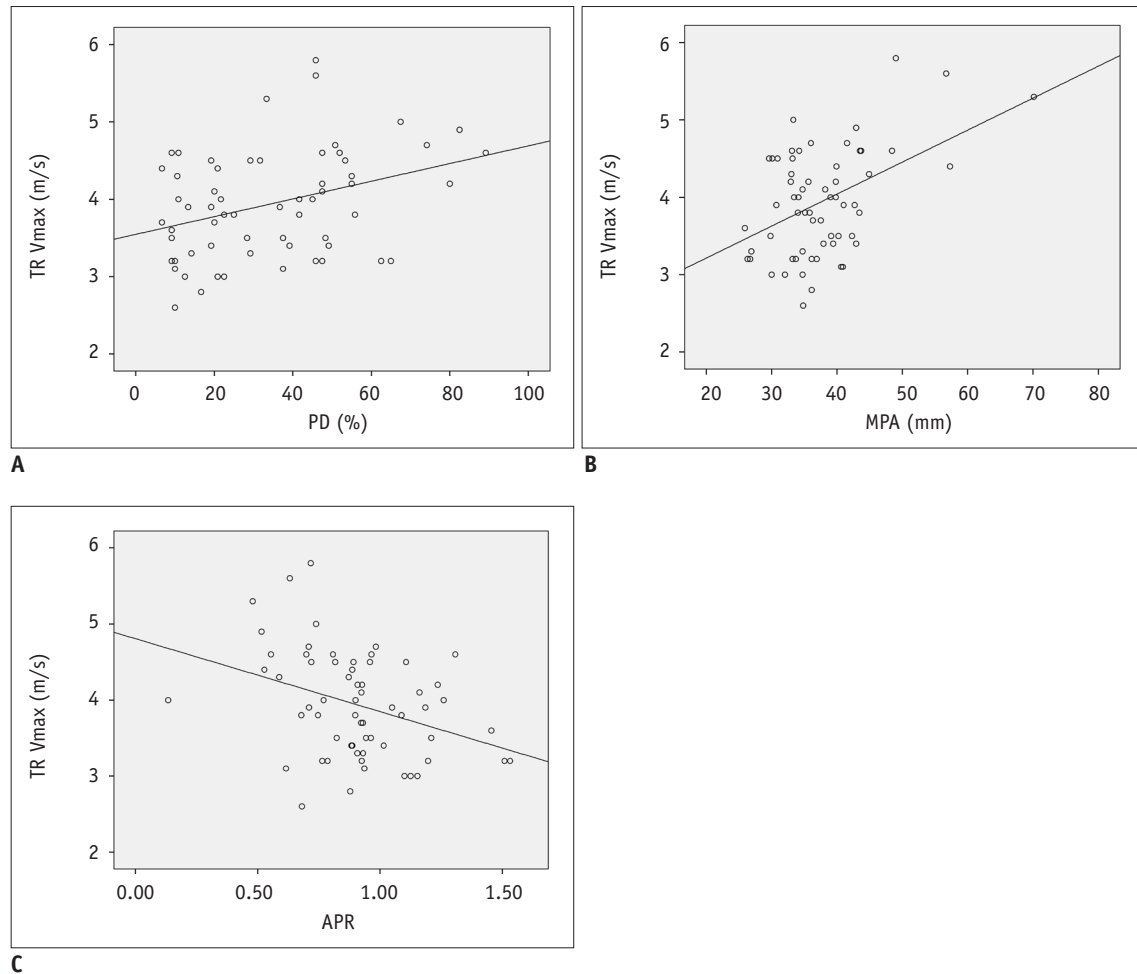


**Fig. 2. Correlations between TR Vmax (m/s) and CT parameters.**

Scatter plots show good correlation between TR Vmax (m/s) and CT parameters, including extent of perfusion defect (PD) (%) (A), diameter of main pulmonary artery (MPA) (mm) (B), and aortopulmonary ratio (APR) (C) in all patients of PHT. PHT = pulmonary hypertension, TR Vmax = maximal velocity of tricuspid regurgitation jet

**Table 3. Multiple Linear Regression Analysis between TR Vmax and Determining CT Parameters**

Multiple Linear Regression	Determining CT Parameters	R <sup>2</sup> Value
All	MPA	0.21
	MPA + PD	0.31
Primary PHT	PD	0.27
	PD + APR	0.40
Secondary PHT	MPA	0.28
	MPA + PD	0.39

**Note.**— APR = aortopulmonary ratio, MPA = diameter of the main pulmonary artery, PD = extent of perfusion defect, PHT = pulmonary hypertension, TR Vmax = maximal velocity of tricuspid regurgitation jet

of pulmonary vasculature, parenchyma and perfusion in patients with CTEPH. Nakazawa et al. (23) revealed that LPBV imaging using DECT for CTEPH is possible for the evaluation of pulmonary perfusion and is comparable

to pulmonary scintigraphy. However, only patients with CTEPH were included in those studies (21, 23). To the best of our knowledge, the present study is the first study to evaluate the differences in perfusion patterns seen on DECT according to the cause of the PHT.

In our study, most of perfusion defects caused by vascular conditions were shown to be wedge-shaped. This pattern is similar to that observed in patients with PTE (16-18). Analysis of specific defect patterns in patients with nonvascular disease causes is complicated owing to the numerous factors that contribute to PHT with complex pathophysiology and physiologic compensation (24, 25). There are several explanations about the pathophysiologic mechanisms of PHT associated with obstructive and restrictive lung diseases. In emphysema, destruction of alveoli and interstitial spaces leads to a loss of pulmonary vessels, causing a decrease in perfusion (25, 26).

Physiologic vasoconstriction due to sustained alveolar hypoxia, followed by vascular remodeling and compression of alveolar vessels by increased intra-alveolar pressures, resulting in increased resistance also show an important impact on PHT in COPD (26, 27). PHT in restrictive lung diseases is reported to occur in as many as 46% of the cases, in idiopathic interstitial pneumonia especially (28, 29). Pulmonary artery dilatation may occur as in patients with primary PHT. However, the severity of main pulmonary arterial dilatation seen on CT is not a reliable indicator of PHT in patients with pulmonary fibrosis (30). PHT in patients with fibrotic lung disease is a reflection of pathologic processes such as small-vessel remodeling as well as a consequence of fibrotic obliteration of the pulmonary vasculature (29, 30). In our study, there were 5 congestive heart failures, 2 dilated cardiomyopathy, 1 Eisenmenger syndrome and 1 valvular heart disease in the cardiogenic group. PHT due to left heart disease is a common consequence of chronic left atrial hypertension in heart failure caused by myocardial and valvular heart disease and is known to be the most common cause of PHT. PHT due to left heart disease promote cascade damaging anatomic and functional changes of pulmonary arterial, capillary and venous circulation, finally accelerating right ventricular (RV) dysfunction and failure (31). Several authors showed for patients with left heart disease that there were perfusion defects in the lower zone, symmetrically on the pulmonary ventilation/perfusion nuclear scans, which were caused by redistribution of pulmonary blood flow (32). PHT due to cardiac causes, i.e., Eisenmenger syndrome, are present in patients with congenital heart diseases such as ventricular septal defect, atrial septal defect and patent ductus arteriosus. The exact pathophysiology for the appearance of PHT in patients with heart defects is not known yet (33).

Chae et al. (18) demonstrated that a combined assessment of perfusion and vascular occlusion may be useful in order to gain a better understanding of the pulmonary embolism (PE) severity. In their study, areas were found in which the perfusion defect and vascular obstruction were mismatched. The investigators explained these mismatches may represent disturbances of the microcirculation or normal perfusion in an area of partial occlusion. Their study showed that DECT perfusion imaging can predict the regional perfusion status as well as patient outcomes. However, Chae et al. (18) focused on acute PE patients and a correlation between the perfusion score and the results of other imaging techniques such as perfusion scintigraphy

or echocardiography as a reference was not evaluated. Several previous studies reported with controversial results about the relationship between the dilatation of MPA and the severity of PHT (14, 15). Renard et al. (22) reported that DECT demonstrates correlations between the severity of pulmonary arterial obstruction and perfusion impairment in patients with CTEPH. Also these links are affected by the development degree of the systemic collateral supply.

It is widely accepted that Doppler echocardiography is an essential component of the diagnostic algorithm of PHT as it makes it possible to confirm the diagnosis. In daily practice TR Vmax is a useful indicator to measure the RV systolic pressure, which is the most accurate echocardiographic method and thought to be an equivalent to pulmonary artery systolic pressure in the absence of pulmonary stenosis (10). It can be calculated from the systolic transtricuspid gradient using the Bernoulli equation (34). Thereafter the estimated right atrial pressure will be added (6, 34). Several studies reported that TR Vmax had a strong positive correlation (0.57 to 0.93) with pulmonary artery systolic pressure measured in right-heart catheterization and the Doppler-estimated pulmonary artery systolic pressure had a high sensitivity (0.79–1.00) and specificity (0.6–0.98) to detect PHT (6–10).

Our results demonstrate the close relationship between TR Vmax and the CT parameters (including PD, MPA, and APR). However, the PD and the MPA did not correlated with each other. Both parameters were also found to be independent determinants of TR Vmax on multiple linear regression analysis. If we assume that a perfusion defect reflects microcirculation alteration and that dilatation of the main pulmonary artery indicates structural arterial change, we might consider that these two elements contribute in different ways to the severity of PHT.

Our study had several limitations. First, the study was retrospective with a relatively small sample size. So it was not possible to avoid bias and the general population cannot be reflected. However, we were able to show the significant correlation between TR Vmax and the CT parameter in this preliminary study. Therefore further prospective studies with larger sample sizes will be required. Second, the CT protocol was fixed with a contrast agent of 100 mL and a scan delay of 20 seconds regardless of individual patient characteristics such as weight or Rt. heart function. Third, we used TR Vmax as a reference standard for PHT rather than the direct measurement of pulmonary arterial pressure in right-heart catheterization. However,



right-heart catheterization is not routinely performed in clinical practice and the reliable accuracy and feasibility of TR Vmax as a substitute for direct measurement has been reported in many published studies (6-9, 33, 35). Fourth, the technical limitations of DECT were a limitation factor as due to the smaller detector width of the 80 kV system, data displayed inside the limited FOV (260 mm) were used for dual-energy reconstruction only. Nevertheless, the FOV included almost all lungs in most of our patients, and in some large patients the far peripheral portion was excluded from evaluation. The iodine enhancement seen on the perfusion map does not reflect all the diverse aspects of pulmonary perfusion, such as regional flow, transit time and regional blood volume. In addition, the systemic blood supply from the bronchial artery or from other collateral vessels cannot be excluded from the perfusion images. However, this is the innate nature of perfusion CT and our purpose was to evaluate perfusion defects in the clinical setting. Finally, interpretation of a perfusion pattern and its extent may be subjective, although our study indicated reliable agreement between two readers.

In conclusion, different perfusion patterns are noted on DECTA of PHT according to the types and causes. The extent of the perfusion defect and the degree of dilatation of the main PA correlate well with the TR Vmax on the echocardiography. The severity of the PHT is more accurately and completely explained by combining the information regarding the perfusion defect and the vascular diameter change.

## REFERENCES

1. Powe JE, Palevsky HI, McCarthy KE, Alavi A. Pulmonary arterial hypertension: value of perfusion scintigraphy. *Radiology* 1987;164:727-730
2. Ogawa Y, Nishimura T, Hayashida K, Uehara T, Shimonagata T. Perfusion lung scintigraphy in primary pulmonary hypertension. *Br J Radiol* 1993;66:677-680
3. Bartalena T, Oboldi D, Guidalotti PL, Rinaldi MF, Bertaccini P, Napoli G, et al. Lung perfusion in patients with pulmonary hypertension: comparison between MDCT pulmonary angiography with minIP reconstructions and 99mTc-MAA perfusion scan. *Invest Radiol* 2008;43:368-373
4. Kumar AM, Parker JA. Ventilation/perfusion scintigraphy. *Emerg Med Clin North Am* 2001;19:957-973
5. McLaughlin VV, Archer SL, Badesch DB, Barst RJ, Farber HW, Lindner JR, et al. ACCF/AHA 2009 expert consensus document on pulmonary hypertension a report of the American College of Cardiology Foundation Task Force on Expert Consensus Documents and the American Heart Association developed in collaboration with the American College of Chest Physicians; American Thoracic Society, Inc.; and the Pulmonary Hypertension Association. *J Am Coll Cardiol* 2009;53:1573-1619
6. Yock PG, Popp RL. Noninvasive estimation of right ventricular systolic pressure by Doppler ultrasound in patients with tricuspid regurgitation. *Circulation* 1984;70:657-662
7. Barst RJ, McGoon M, Torbicki A, Sitbon O, Krowka MJ, Olschewski H, et al. Diagnosis and differential assessment of pulmonary arterial hypertension. *J Am Coll Cardiol* 2004;43(12 Suppl S):40S-47S
8. Bossone E, Citro R, Blasi F, Allegra L. Echocardiography in pulmonary arterial hypertension: an essential tool. *Chest* 2007;131:339-341
9. Bossone E, Bodini BD, Mazza A, Allegra L. Pulmonary arterial hypertension: the key role of echocardiography. *Chest* 2005;127:1836-1843
10. Bossone E, D'Andrea A, D'Alto M, Citro R, Argiento P, Ferrara F, et al. Echocardiography in pulmonary arterial hypertension: from diagnosis to prognosis. *J Am Soc Echocardiogr* 2013;26:1-14
11. Engelke C, Schaefer-Prokop C, Schirg E, Freihorst J, Grubnic S, Prokop M. High-resolution CT and CT angiography of peripheral pulmonary vascular disorders. *Radiographics* 2002;22:739-764
12. Rossi A, Attinà D, Borgonovi A, Buia F, De Luca F, Guidalotti PL, et al. Evaluation of mosaic pattern areas in HRCT with Min-IP reconstructions in patients with pulmonary hypertension: could this evaluation replace lung perfusion scintigraphy? *Eur J Radiol* 2012;81:e1-e6
13. Kuriyama K, Gamsu G, Stern RG, Cann CE, Herfkens RJ, Brundage BH. CT-determined pulmonary artery diameters in predicting pulmonary hypertension. *Invest Radiol* 1984;19:16-22
14. Ng CS, Wells AU, Padley SP. A CT sign of chronic pulmonary arterial hypertension: the ratio of main pulmonary artery to aortic diameter. *J Thorac Imaging* 1999;14:270-278
15. Tan RT, Kuzo R, Goodman LR, Siegel R, Haasler GB, Presberg KW. Utility of CT scan evaluation for predicting pulmonary hypertension in patients with parenchymal lung disease. Medical College of Wisconsin Lung Transplant Group. *Chest* 1998;113:1250-1256
16. Fink C, Johnson TR, Michaely HJ, Morhard D, Becker C, Reiser M, et al. Dual-energy CT angiography of the lung in patients with suspected pulmonary embolism: initial results. *Rofa* 2008;180:879-883
17. Hoey ET, Gopalan D, Ganesh V, Agrawal SK, Qureshi N, Tasker AD, et al. Dual-energy CT pulmonary angiography: a novel technique for assessing acute and chronic pulmonary thromboembolism. *Clin Radiol* 2009;64:414-419
18. Chae EJ, Seo JB, Jang YM, Krauss B, Lee CW, Lee HJ, et al. Dual-energy CT for assessment of the severity of acute pulmonary embolism: pulmonary perfusion defect score compared with CT angiographic obstruction score and



- right ventricular/left ventricular diameter ratio. *AJR Am J Roentgenol* 2010;194:604-610
19. Lee CW, Seo JB, Song JW, Kim MY, Lee HY, Park YS, et al. Evaluation of computer-aided detection and dual energy software in detection of peripheral pulmonary embolism on dual-energy pulmonary CT angiography. *Eur Radiol* 2011;21:54-62
  20. Pontana F, Remy-Jardin M, Duhamel A, Faivre JB, Wallaert B, Remy J. Lung perfusion with dual-energy multi-detector row CT: can it help recognize ground glass opacities of vascular origin? *Acad Radiol* 2010;17:587-594
  21. Hoey ET, Mirsadraee S, Pepke-Zaba J, Jenkins DP, Gopalan D, Screaton NJ. Dual-energy CT angiography for assessment of regional pulmonary perfusion in patients with chronic thromboembolic pulmonary hypertension: initial experience. *AJR Am J Roentgenol* 2011;196:524-532
  22. Renard B, Remy-Jardin M, Santangelo T, Faivre JB, Tacelli N, Remy J, et al. Dual-energy CT angiography of chronic thromboembolic disease: can it help recognize links between the severity of pulmonary arterial obstruction and perfusion defects? *Eur J Radiol* 2011;79:467-472
  23. Nakazawa T, Watanabe Y, Hori Y, Kiso K, Higashi M, Itoh T, et al. Lung perfused blood volume images with dual-energy computed tomography for chronic thromboembolic pulmonary hypertension: correlation to scintigraphy with single-photon emission computed tomography. *J Comput Assist Tomogr* 2011;35:590-595
  24. Weitzenblum E, Apprill M, Oswald M, Chauat A, Imbs JL. Pulmonary hemodynamics in patients with chronic obstructive pulmonary disease before and during an episode of peripheral edema. *Chest* 1994;105:1377-1382
  25. Kim BH, Seo JB, Chae EJ, Lee HJ, Hwang HJ, Lim C. Analysis of perfusion defects by causes other than acute pulmonary thromboembolism on contrast-enhanced dual-energy CT in consecutive 537 patients. *Eur J Radiol* 2012;81:e647-e652
  26. Pierson DJ. Pathophysiology and clinical effects of chronic hypoxia. *Respir Care* 2000;45:39-51; discussion 51-53
  27. Grosse C, Grosse A. CT findings in diseases associated with pulmonary hypertension: a current review. *Radiographics* 2010;30:1753-1777
  28. Shorr AF, Wainright JL, Cors CS, Lettieri CJ, Nathan SD. Pulmonary hypertension in patients with pulmonary fibrosis awaiting lung transplant. *Eur Respir J* 2007;30:715-721
  29. Patel NM, Lederer DJ, Borczuk AC, Kawut SM. Pulmonary hypertension in idiopathic pulmonary fibrosis. *Chest* 2007;132:998-1006
  30. Devaraj A, Wells AU, Meister MG, Corte TJ, Hansell DM. The effect of diffuse pulmonary fibrosis on the reliability of CT signs of pulmonary hypertension. *Radiology* 2008;249:1042-1049
  31. Guazzi M, Borlaug BA. Pulmonary hypertension due to left heart disease. *Circulation* 2012;126:975-990
  32. Au VW, Jones DN, Slavotinek JP. Pulmonary hypertension secondary to left-sided heart disease: a cause for ventilation-perfusion mismatch mimicking pulmonary embolism. *Br J Radiol* 2001;74:86-88
  33. Galiè N, Torbicki A, Barst R, Dartevielle P, Haworth S, Higenbottam T, et al. Guidelines on diagnosis and treatment of pulmonary arterial hypertension. The Task Force on Diagnosis and Treatment of Pulmonary Arterial Hypertension of the European Society of Cardiology. *Eur Heart J* 2004;25:2243-2278
  34. Hatle L, Angelsen BA, Tromsdal A. Non-invasive estimation of pulmonary artery systolic pressure with Doppler ultrasound. *Br Heart J* 1981;45:157-165
  35. Arcasoy SM, Christie JD, Ferrari VA, Sutton MS, Zisman DA, Blumenthal NP, et al. Echocardiographic assessment of pulmonary hypertension in patients with advanced lung disease. *Am J Respir Crit Care Med* 2003;167:735-740